IJERMT

International Journal of Engineering Research & Management Technology

ISSN: 2348-4039

May-2019 Volume 6, Issue-3

Email: editor@ijermt.org www.ijermt.org

ELECTRONIC DYNAMICS

Mrs. Seema Devi

Research scholar

Department of Poltical Science

Kurukshetra University, Kurukshetra, Haryana

Abstract

In this review, the dynamics of electrons moving in two dimensions in magnetic potentials with scales of variation that are less than the mean free path are investigated. The physics of microscopically inhomogeneous magnetic fields is related to crucial basic difficulties in the fractional quantum Hall effect, superconductivity, spintronics, and the physics of grapheme, and it spins forth intriguing applications, which will be detailed in this article. Following the presentation of the preliminary work that was carried out on electron localization in random magnetic fields, the presentation moves on to the experimental methods for manufacturing magnetic potentials. Then, the phenomena of drift–diffusion, such as commensurability oscillations, magnetic channeling, resistance resonance effects, and magnetic dots, are explained. After that, we go into some of the quantum phenomena that may occur in magnetic potentials, such as magnetic quantum wires, magnetic minibands in superlattices, rectification caused by snake states, quantum tunnelling, and Klein tunnelling. Spintronics in inhomogeneous magnetic fields is the topic of the third and final portion of this book. This includes electrically produced spin resonance, spin resonance fluorescence, coherent spin manipulation, and spin filtering via magnetic field gradients and circular magnetic fields.

keywords: electrons , magnetic ,grapheme

Introduction

The measurement of the magnetic moment of individual silver atoms by Stern and Gerlach is considered to be the genesis of the application of magnetic fields that change throughout space. In order to generate a macroscopic magnetic field gradient that varied across lengths of centimetres, the researchers' experimental set-up consisted of an electromagnet that was outfitted with asymmetric pole pieces. On the other hand, magnetic impurities allow for the generation of magnetic fields that are variable on atomic sizes. Within the context of the Kondo effect, the behaviour of magnetic impurities is analysed. An important area of research that has arisen over the course of the past decade is known as the study of magnetic fields fluctuating on the scale of the electron mean free path. This is due, in part, to recent developments in technology that have made it possible to fabricate nanomagnets with well-defined geometries, as well as developments in the cultivation of high-mobility two-dimensional electron gases (2DEGs). The challenge of electron localization in a chaotic magnetic field served as the impetus for the investigation of magnetically modulated two-dimensional electron gases (2DEGs). In the presence of a random magnetic field with zero average, the issue that has to be answered is

whether the wavefunction of electrons in two dimensions is extended or confined. The issue is intricately connected to the phenomenon of poor localization in random electrostatic potentials. At 0 Kelvin, the two-dimensional electron gas (2DEG) is an insulator because electrostatic disorder is known to localise electron wavefunctions in both dimensions. The time reversal symmetry of clockwise and anticlockwise interference routes is broken when a homogeneous magnetic field (B) is applied to the 2DEG. This result may be seen as a negative consequence of the application. When Landau levels are formed, all of the electronic states stay confined with the exception of a thin band in the centre of the structure where metallic conduction takes occur. A random magnetic field with zero average will break time reversal symmetry in both the local and the global context. The breakdown of extended states brought about by the random potential a priori offers a reasonable basis to anticipate electron localization and an insulating behaviour in the random magnetic field [1–3]. On the other hand, Zhang and Arovas [4] alluded to the occurrence of magnetic edge states at the borders of positive and negative magnetic field domains [5]. In order to produce globally extended states, these states must first travel across the saddle points of the random magnetic potential and then percolate through the nodes of the network. Accordingly, it would appear that the 2DEG that was modified by a random magnetic field is in reality a metal; this conclusion is corroborated by numerical simulations.

Quantum transport has been experimentally examined in quasi-random magnetic fields where the correlation length of magnetic fluctuations is greater than the electron mean free path. The results of the experiment therefore contradict the theoretical scenario discussed before. In its place, the 2DEG acts as if it were a network of diffusive magnetic domains, each of which has its own local Hall resistivity. In this particular instance, theoretical calculations forecast a V-shaped magnetoresistance, which is supported by experimental findings. Patterning type II superconductors on top of 2DEGs was the first method that was used in order to construct magnetic field profiles that varied on scales that were smaller than the mean free path. In this particular instance, the vortex lattice weaves the 2DEG with a hexagonal array of magnetic spots that are spaced 50 nm/[B(T)] 1/2 apart from one another (Al films). The positive magnetoresistance is caused by the small angle deflection of ballistic electrons that is caused by the magnetic patches. When the wavelength of Fermi electrons is matched to the distance between vortices, an effect known as electron diffraction may be seen. This effect was confirmed who observed a maximum adjustment to the Hall resistance when the circumstances were those of diffraction. Magnetic field profiles with a high amplitude but a zero-mean average have been established throughout the course of the last decade and a half. In this section, we will go through the electron and electron spin dynamics that occur in these potentials. In this presentation, various illustrations of the significance of magnetic edge states for both fundamental physics and practical applications will be presented. It describes landmark findings, such as the first demonstration of lateral magnetic superlattices and the first coherent control of the electron spin, among other achievements in the field.

Elementary Electron Dynamics

There are many different aspects of the dynamics of electrons that may be described, and most likely should be presented, as background information before looking at the interaction of dispersed electronwaves. A small portion of them will be discussed in this section, with the primary focus being placed on fundamental ideas that are pertinent to the principles that will be developed on in subsequent chapters. The fundamentals of both the special theory of relativity and classical mechanics are summarised because all of the topics that are discussed throughout the text are dependent on classical

mechanics (section 3.1) and without exception, they are consistent with the special theory of relativity (section 3.2). In addition to reviewing the fundamental concepts of relativistic classical dynamics, in Section 3.3, we consider some of the methods of electron generation and discuss the Child-Langmuir law, which places a limit on the maximum current that can be achieved by applying a voltage to a cathode. Both of these topics are covered after we have reviewed the fundamental concepts of relativistic classical dynamics. Once electrons have been created, they are often directed to the interaction zone by magnetic fields and waveguides once they have been produced. In the following section (3.4), we will cover some of the fundamentals of beam propagation in free space with a periodic or uniform magnetic field. The section comes to a close by discussing the fundamental parameters that characterise beam quality: emittance and brightness. The topic of space-charge waves is discussed in Section 3.5. Following an explanation of the fundamental ideas behind fast and slow space-charge waves, we will examine two types of instability that may manifest themselves when these waves are present. Both the resistive wall instability and the two-beam instability are types of the same instabilities. It has been demonstrated that the interference of two space-charge waves plays the most important function in relativistic klystrons. A quick explanation on radiation caused by moving charges serves as the final topic of Chapter 3. (Sect. 3.6).

Classical Dynamics

Because it is possible to adequately characterise the electron-wave interaction within the framework of classical physics in a significant portion of the interaction schemes, we will not be discussing the impacts of quantum mechanics at this time. The Newtonian equation of motion, the Lagrangian formalism, or the Hamiltonian formalism are the three main components of the classical method. The relativistic framework is taken into consideration in every scenario. Furthermore, in every scenario of interest, a large number of particles are in play; as a result, statistical techniques are called into play. It is for this reason that we will now present in a very condensed form the kinetic and the fluid approximations, both of which are utilised throughout the text.

Newtonian Equations of Motion

The elementary equations, which describe the dynamics of a particle at the classical level, are given by

$$\frac{\mathrm{d}}{\mathrm{d}t}\left[m\gamma(t)\mathbf{v}(t)\right]=\mathbf{F}(t),$$

where F( )t is the force acting on the particle and if an electromagnetic field is present then the force is given by the Lorentz force which reads

$$\mathbf{F}(t)=-e\left\{\mathbf{E}[\mathbf{r}(t),t]+\mathbf{v}(t)\times\mathbf{B}[\mathbf{r}(t),t]\right\};$$

e and m represent the charge and the rest mass of the electron respectively, v( )t is its velocity vector at any point in time and

$$\gamma(t)=\frac{1}{\sqrt{1-\mathbf{v}(t)\cdot\mathbf{v}(t)/c^2}}.$$

The electromagnetic field, $\mathbf{E}(\mathbf{r}(t),t)$ and $\mathbf{B}(\mathbf{r}(t),t)$ is the field at the particle's location.

It is necessary to ascertain the position of the particle at each instant in time in order to provide a comprehensive description of the dynamics of the particle; this information is provided by.

$$\frac{\mathrm{d}}{\mathrm{d}t}\mathbf{r}(t)=\mathbf{v}(t).$$

The state-vector of such a particle is a 6D vector and it consists of the relative location of the particle r( )t and its momentum i.e $[\mathbf{r}(t),m\gamma(t)\mathbf{v}(t)]$.

These equations allow for the conservation of energy to be determined, much like it was possible to do with Maxwell's equations. In order to do this, (3.1.1) is scaled up by multiplying it by v()t. After substituting (3.1.2) into the right-hand side, we are able to find that the second term contribution is identically zero because the product v B is orthogonal to both the velocity vector and the magnetic induction. This allows us to conclude that the second term contribution is identically zero. On the left, we can see the following:

$$\begin{aligned}&m\mathbf{v}(t)\cdot\frac{\mathrm{d}}{\mathrm{d}t}[\gamma(t)\mathbf{v}(t)]\\&\quad=m\frac{1}{2}\gamma(t)\frac{\mathrm{d}}{\mathrm{d}t}[\mathbf{v}(t)\cdot\mathbf{v}(t)]+m[\mathbf{v}(t)\cdot\mathbf{v}(t)]\frac{\mathrm{d}}{\mathrm{d}t}\gamma(t),\end{aligned}$$

which can be simplified if we now use the definition of γ ( )t in (3.1.3) to express v v· as 2 2 c t [1 ( )] γ− − which yields

$$mc^2\frac{\mathrm{d}}{\mathrm{d}t}\gamma(t)=-e\mathbf{v}(t)\cdot\mathbf{E}[\mathbf{r}(t),t].$$

This is the expression for single particle energy conservation.

Lagrangian Formalism

When attempting to formulate the dynamics of a single particle, it is helpful to apply a different technique in many different situations since it is more convenient. The fundamental concept is to define a scalar function denoted by the letter L as the Lagrangian, and then construct the vector equation of motion using L as the starting point. This function is dependent on the particle's velocity as well as its position, and in general, it may also be dependent on the passage of time. We may, without sacrificing any sense of generality, describe the action as

$$I=\int_{t_1}^{t_2}\mathrm{d}tL(\mathbf{v},\mathbf{r};t),$$

Hence it is necessary that the velocity of the particle from time 1 t to time 2 t be such that the line integral is an extremum for the route that the particle is travelling. In order to give a mathematical shape to this assertion, it must be required that the action in question be at an extreme point with regard to a virtual change denoted by r, hence.

$$\delta I = \delta \int_{t_1}^{t_2} dt L(\mathbf{v}, \mathbf{r}; t) = 0,$$
$$= \int_{t_1}^{t_2} dt \delta L(\mathbf{v}, \mathbf{r}; t) = 0,$$
$$= \int_{t_1}^{t_2} dt \left[\frac{\partial L}{\partial \mathbf{r}} \delta \mathbf{r} + \frac{\partial L}{\partial \mathbf{v}} \frac{d}{dt} \delta \mathbf{r} \right] = 0$$
$$= \int_{t_1}^{t_2} dt \delta \mathbf{r} \left[\frac{\partial L}{\partial \mathbf{r}} - \frac{d}{dt} \frac{\partial L}{\partial \mathbf{v}} \right] = 0,$$

When we refer to "virtual" in this situation, we are referring to an infinitesimal change in the configuration space that is caused by an infinitesimal change in the coordinates system, r, and that change is compatible with the forces that are being applied to the particle at the current moment. We made advantage of the fact that, following the integration by parts, the variation at 1 t and 2 t is exactly zero, in the final line of the formula that was shown earlier. Therefore, in order to achieve the desired result of I = 0, the Lagrangian has to be a solution to the differential equation that is presented below.

$$\frac{d}{dt}\left(\frac{\partial L}{\partial \mathbf{v}}\right) - \frac{\partial L}{\partial \mathbf{r}} = 0.$$

This is called Lagrange's equation and it is identical with the (relativistic) equations of motion, provided that L is chosen to be

$$L = mc^2 \sqrt{1 - \mathbf{v} \cdot \mathbf{v} / c^2} + e(\Phi - \mathbf{v} \cdot \mathbf{A}),$$

where Φ is the scalar electric potential and A is the magnetic vector potential. At this point, we are in position to define in a systematic way the momentum of a particle in the presence of an electromagnetic field. This will be referred to as the canonical momentum associated with the coordinate r and it is defined by

$$\mathbf{p} = \frac{\partial L}{\partial \mathbf{v}} = m \frac{\mathbf{v}}{\sqrt{1 - \mathbf{v} \cdot \mathbf{v} / c^2}} - e\mathbf{A} = m\gamma \mathbf{v} - e\mathbf{A}.$$

By keeping this concept and the Lagrange equation in mind, we are already able to bring out one of the benefits of the Lagrangian formalism. The second component in equation (3.1.9) disappears if L is not an explicit function of one of the coordinates (let's say x). When taken together, these two definitions give rise to the conclusion that the relevant component of the canonical momentum, which in this instance is denoted by the letter x p, is a constant of motion. Because of this, the constants of motion may be determined by deducing them from the symmetry of the system.

Electron Generation

The electrons are not confined in any of the interaction processes that are going to be covered in this chapter. However, in the natural world electrons are bound to atoms or molecules; hence, in order to remove electrons from a substance and put them to use in the process of energy conversion, the material must be broken down. In this part, we will discuss a few different aspects that are related to the production of free electrons. There are a number of methods that may be utilised in order to liberate electrons from the bulk material. One of these methods is known as field-emission, and it

involves the application of an electric field that is perpendicular to the metal vacuum interface. A resurgence of interest in this idea might be attributed to the fact that it is theoretically possible to construct microscopic tips (on a size of sub-microns) utilising microelectronics technology. The current density may become quite considerable with this method, despite the fact that individual tips only generate very modest currents. This is because the method allows for the fabrication of many such tips on a single square centimetre. In comparison to other field-emitters, the voltage that is applied is quite modest. The thermionic emission technique is an additional approach for the extraction of electrons. In this scenario, the emitting surface, which is the cathode, gets heated, and as a result, a portion of the material's electrons are able to triumph over the work function, which allows them to become free. The process of photo-emission is the basis for the third mechanism. In this scenario, the cathode is illuminated by a laser beam, and the photons emitted by the beam provide the electrons with enough energy to surpass the work function. The emission of electrons from metallic points that are in close proximity to dielectric materials is the basis of the fourth mechanism. A fifth potential method depends on something that is known as secondary emission. In this scenario, one electron meets a surface, which then releases other electrons into the surrounding space. In the next subsections, we will discuss various different themes that are connected to the production of electrons.

Field Emission from a Rough Surface

$$J[\mathrm{A}/cm^2] = \frac{1.54\cdot 10^{-6} E^2}{\varphi t^2\left(3.79\cdot 10^{-4}\frac{\sqrt{E}}{\varphi}\right)} \exp\left[-6.83\cdot 10^{7}\frac{\varphi^{3/2}}{E}\mathrm{v}\left(3.79\cdot 10^{-4}\frac{\sqrt{E}}{\varphi}\right)\right]$$

where E cm [V /] denotes the electric field, the work function is denoted by ϕ[e] V and the two other functions can be approximated by 1.6897 v( ) 1 u u − , 1.3343 tu u ( ) 1 0.1107 + . This represents an ideal situation whereby the emitting surface is of zero roughness. In practice, the surface has a finite roughness and as a result the local field is enhanced by a geometric representing the microprotrusion therefore locally, we may expect current density enhancement. At the macroscopic level, namely after averaging over all microscopic deviations from ideal flatness, the emission may be corrected by replacing the local electric field (E) by an enhancement factor β or explicitly, E E → β .

In this part, we analyse an idealised model to characterise the random micro-protrusions in terms of a corrugated surface. This is done for the purpose of proving the influence that such a geometry has on the overall nature of the emission. A number of researchers [Miller (1967), Miller (1984), Lewis (1955), and Chattron (1966)] have investigated the influence that different geometric configurations have on the emission of electrons, with the primary focus being placed on determining the geometric enhancement factor of a single emitter. Even when numerous emitters are involved, such as in the case of arrays of field emitters, each tip is still isolated and controlled separately. As a result, the coupling effect between nearby tips may be overlooked while operating in zero order. When the coupling is taken into account, there are some grating characteristics that make it easier to generate the maximum current, while others contribute to the development of the largest current density. It is necessary to keep in mind that once the tips are separated, the electric field may be large, and as a result, the current density at its peak is high; however, the total current generated in a unit length of the structure is small because the emitting area is so small. This is important to keep in mind so that we can visualise the reason for such a maximum to occur. At the opposite end of the spectrum, if the tips are very close to

one another, they have an effect on one another, the electric field (at the tip) is quite modest, and once again, the total current created in a unit length is minimal, despite the emitting area being somewhat bigger. It is anticipated that the current will reach its maximum value somewhere in between these two low numbers.

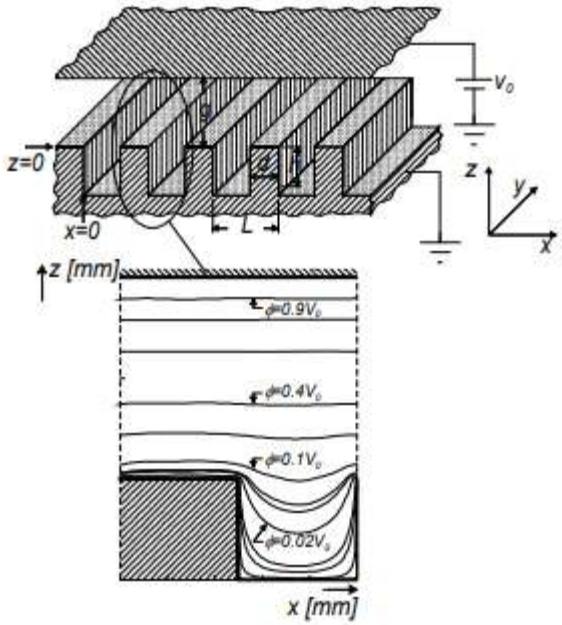

Fig. 3.2: Schematic of the system is presented in the top-frame. In the lower frame typical potentialcontours are illustrated (for L = 1 mm, h = 1 mm, d = 0.5 mm and g = 1 mm)

Experimental strategies for making inhomogeneous magnetic fields

Constructing micromagnets close to a two-dimensional electron generator (2DEG) is one strategy for producing a magnetic field that is microscopically inhomogeneous. Ballistic electrons are steered away from their path by a local Lorentz force, which is applied by a stray magnetic field. If the magnetization M is homogenous, then the magnetic modulation profile may be computed to an extremely high degree of precision . Either by employing hard uniaxial magnets like SmCo5 or by saturating the magnetization with an external magnetic field, one can achieve uniform magnetization in their material. Imaging using an AFM may also be used to measure the size of micromagnets to an extremely high degree of accuracy. It is known that the thickness of the buffer layer that sits between the 2DEG and the micromagnet is on the order of an atomic monolayer at most. Due to the availability of these data, a precise calculation of the stray magnetic field at the location of the 2DEG may be made. Take, for example, the one-dimensional magnetic superlattice that is seen in figure 1. (a). The GaAs/AlGas heterojunction that is buried z0 depths below the surface is modulated by a grating made of finger gates made of cobalt. The Fourier transformation of Maxwell's equations may be used to readily calculate the stray magnetic field that is produced by an array that is periodic One obtains.

$$B_{1,x}(x, z_0) = \mu_0 M \frac{hd}{a} \sum_{n=1}^{\infty} q_n F(q_n) e^{-q_n(z_0+h/2)} \sin(q_n x - \theta),$$

$$B_{1,y}(x, z_0) = 0,$$

$$B_{1,z}(x, z_0) = \mu_0 M \frac{hd}{a} \sum_{n=1}^{\infty} q_n F(q_n) e^{-q_n(z_0+h/2)} \cos(q_n x - \theta),$$

where qn = 2πn/a, a is the period of the array, h the height of the cobalt fingers and d their width, θ is the tilt angle of the magnetization and

$$F(q_n) = \frac{\sin(q_n d/2)}{(q_n d/2)} \frac{\sinh(q_n h/2)}{(q_n h/2)},$$

is the form factor of rectangular stripes. Since electron motion is confined to the plane, magnetoresistive effects will only

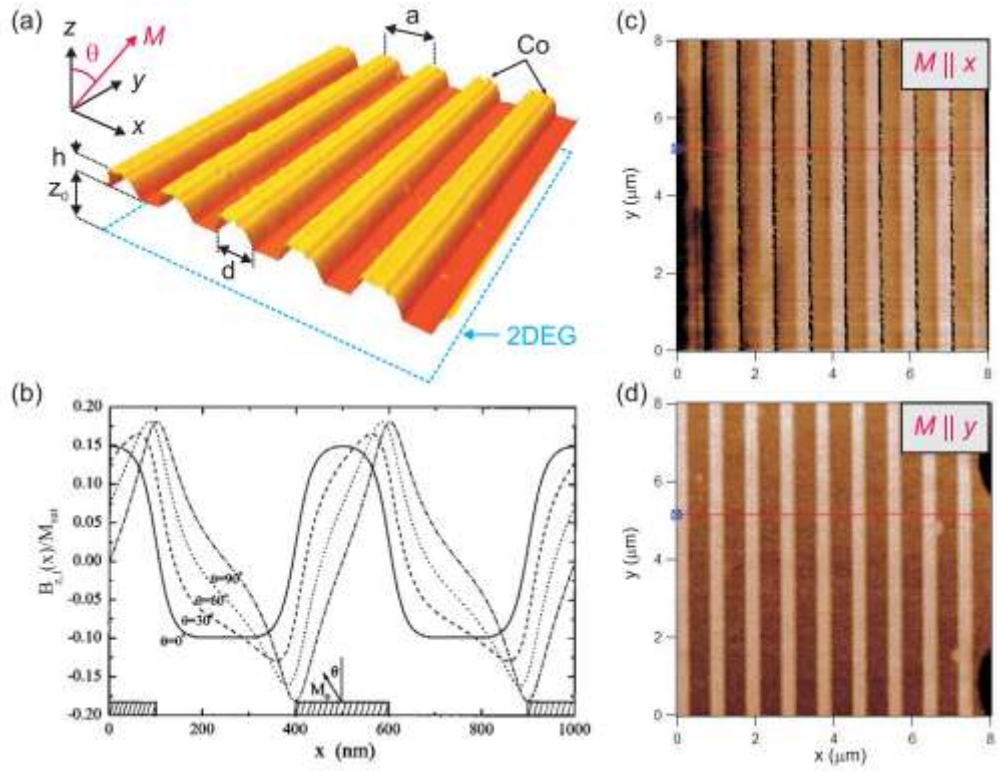

Figure 1. (a) Cobalt finger gates at the surface of a 2DEG. (b) Magnetic modulation profiles at different tilt angles of the magnetization. (c) MFM image of the cobalt grating magnetized along the short axis of the stripes, in the plane of the 2DEG. The magnetic poles appear as the black lines. (d) MFM image of the grating magnetized along the long axis. The magnetic poles are absent. Parameters: a = 400 nm, d = 200 nm, h = 160 nm and z0 = 90 nm.

rely on the component of the perpendicular magnetic field called B1,z, which may be seen shown in figure 1. (b). The geometry of the magnetic field modulation shifts from a rectangular to a triangular configuration whenever the magnetization rotates from normal to in-plane (x). The magnetization of cobalt is 0Ms = 1.82 T after it has reached its saturation point, which results in a modulation amplitude

of 0.3 T. When the grating is magnetised in the y-direction, the magnetic modulation can be turned off. Experimenters will find this gadget to be quite helpful for displaying the effects of magnetic modulation in their experiments. Panel c displays the MFM pictures of the grating when the magnetization is aligned along the short axis of the stripes, and panel d displays them when the magnetization is aligned along the long axis of the stripes. Take note of the fact that the development of magnetic poles in the first scenario corresponds to the condition in which a magnetic modulation is applied to the magnetic field. The Meissner effect can also be utilised with superconducting components in order to achieve the desired screening of the applied magnetic field. However, the screening process is made more difficult by the fact that the vast majority of type I superconductors, such as lead, show type II superconductivity when they are put down in thin layers. The magnetization of the superconducting element is described by the equation 0M = B when it is below the first critical field, Bc1. To calculate the stray magnetic field that is produced by a 1D superconducting grating, replace all instances of 0M with B in the relevant equations (1). In the region between the first and second critical fields, the modulation is weakened as a result of the penetration of vortex lines from the margins of the superconductor. The intensity of the magnetic modulation is progressively less as B gets higher, until it completely disappears at Bc2. When Bc1 is less than B and Bc2 is more than B, the pinning of vortices plays a significant role because the sign of magnetic modulation is different depending on whether the external magnetic field is increased or decreased. The flux lines that are stuck inside the superconductor are unable to simply move outside of the material when the magnetic field strength is decreased. On the other hand, as the magnetic field strength is increased, it becomes more difficult for the flux lines to enter the interior. When the sweep direction is changed from up to down, there is a change of in the phase of the magnetic modulation. This shift is caused by the pinning of vortices. The production of fringing magnetic fields by running a current through a metal stripline is something that has been theoretically studied [18] and is something that is realised in the MRAM technology. However, because semiconductor heterojunctions impose a buffer layer between the stripline and the 2DEG, this method is not an effective method for producing inhomogeneous magnetic fields. Over this buffer layer, the stray magnetic field decays to levels that are negligible, so the method is ineffective. In most cases, parasitic electrostatic modulations will appear alongside the magnetic modulations that are created by the aforementioned approaches. As the sample is cooled down to cryogenic temperatures, they result from the accumulation of strain at the interface between the metal and the semiconductor. The piezoelectric potential of polar semiconductors like GaAs is on the order of a millivolt. Magnetostriction in the ferromagnet may also affect the piezoelectric potential to the point that the magnetization curve may be identified based only on voltage measurements. This phenomenon is illustrated in figure 2, which depicts the modulation of a two-dimensional hole gas by a dysprosium stripe. At 1.7 K, the piezovoltage displays a hysteresis curve that is analogous to the magnetization curve of dysprosium. This is due to the fact that the thermal activation of holes occurs at this temperature.

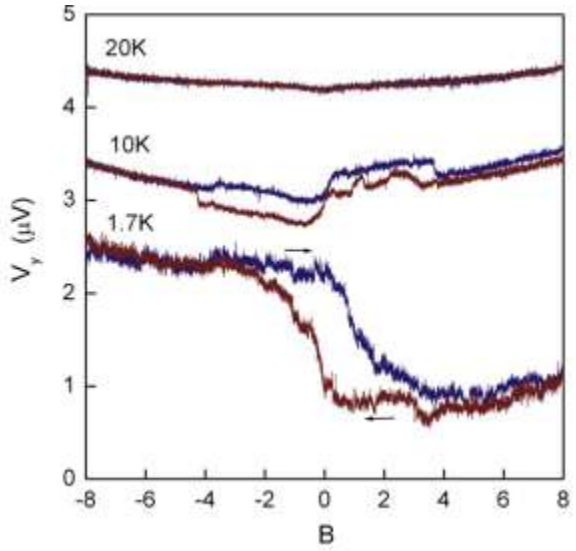

Figure 2. The piezo-magnetostrictive effect. A finite piezoelectric voltage is measured across a 2D hole gas modulated by a dysprosium finger gate. The stripe, at the centre of the Hall bar, applies variable strain to the semiconductor through magnetostriction. The magnetization curve of dysprosium is detected in the piezo-voltage. No current is applied. The finger gate is magnetized along its short axis and in the plane.

20 K is sufficient to screen the piezoelectric potential causing the hysteresis curve to vanish. Taking the magnetostrictive constant of dysprosium as $\varepsilon y = 10.6 \times 10{-}3$ and the valence band deformation potential as = 2.7 eV, the maximum piezo-voltage is Vy = 1.6 mV. The residual electrostatic modulation may be attenuated by aligning stripes with the [100] crystallographic axes or by equalizing the distribution of strain with a metal gate.

Non-planar two-dimensional electron gases

Another approach to getting magnetic steps is to overgrow GaAs/AlGas heterojunctions on non-planar substrates. This is one way to get magnetic steps. The Hall bar shown in figure 3(a) has an etched facet built into it, which was used to re-grow the 2DEG. Due to the fact that the magnetic modulation is the vector component that is perpendicular to the 2DEG, an external magnetic field that is applied in the plane will result in a modulation field that is infinite in the facet and zero everywhere else. have expanded on this concept by applying it to cylindrical 2DEGs (see pictures 3(b)) (d). To get a sinusoidal modulation, they micromachined a free standing 2DEG and wrapped it up around a cylinder. This gave them the desired effect. Foden et al [23] have successfully computed the electrical band structure that should be expected to correspond to this shape. Making magnetic modulations of any size requires non-planar structures, which are desirable for this purpose.

Chern–Simons effective magnetic field

In the fractional quantum Hall effect near filling factor $\nu = 1/2$, the system of strongly correlated electrons is equivalent to non-interacting composite fermions with a well defined Fermi surface. A composite fermion consists of an electron paired with two flux quanta which oppose the applied magnetic field.

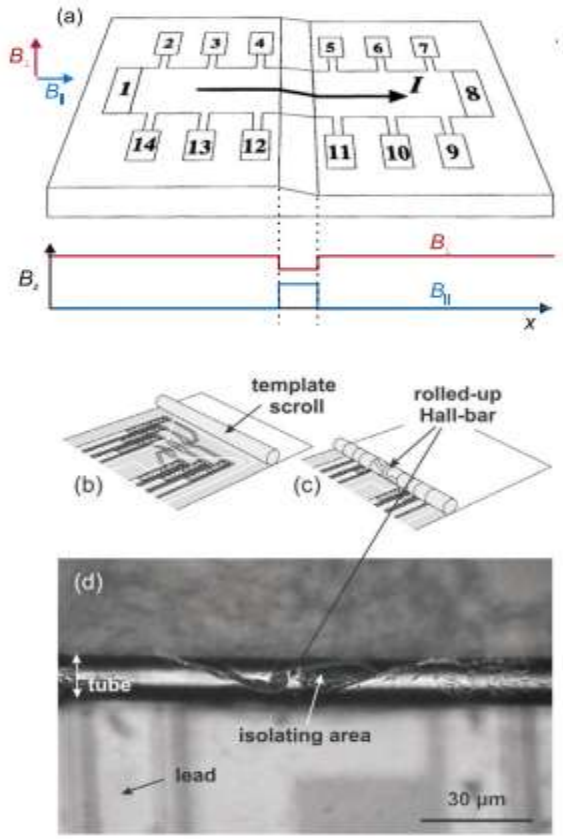

Figure 3. Inhomogeneous magnetic fields in non-planar 2DEGs: (a) GaAs/AlGaAs heterojunction grown on a step etch and fabricated as a Hall bar; (b)–(d) micromachined and rolled-up Hall bars. Reproduced with permission from [22]. Copyright 2006, American Institute of Physics.

Beff is equal to (1 + 2v)B and represents the effective field that is encountered by composite fermions. A spatial modulation of the electron concentration is comparable to a spatial modulation of the effective magnetic field. This is because relies on the local electron concentration ns(x) by the equation (x) = ns(x)(h/eB). Direct evidence for the effective modulation field may be found in the observations of commensurability oscillations and the channelling of composite fermions in snake orbits.

Conclusion

The measurement of the magnetic moment of individual silver atoms by Stern and Gerlach is considered to be the genesis of the application of magnetic fields that change throughout space. In order to generate a macroscopic magnetic field gradient that varied across lengths of centimetres, the researchers' experimental set-up consisted of an electromagnet that was outfitted with asymmetric pole pieces. electrons in two dimensions moving through magnetic potentials that change on scales that are less than their mean free path. The physics of microscopically inhomogeneous magnetic fields is related to crucial basic difficulties in the fractional quantum Hall effect, superconductivity, spintronics, and the physics of graphene, and it spins forth intriguing applications, which will be detailed in this article. Following the presentation of the preliminary work that was carried out on electron localization in random magnetic fields, the presentation moves on to the experimental methods for manufacturing magnetic potentials.

References

1. Lee D K K, Chalker J T and Ko D Y K 1994 Localization in a random magnetic field: the semiclassical limit Phys. Rev. B 50 5272
2. Yakubo K and Goto Y 1996 Localization of two-dimensional electrons in a random magnetic field Phys. Rev. B 54 13432
3. Sugiyama T and Nagaosa N 1993 Localization in a random magnetic field Phys. Rev. Lett. 70 1980
4. Zhang S C and Arovas D P 1994 Effective field theory of electron motion in the presence of random magnetic flux Phys. Rev. Lett. 72 1886
5. M¨uller J E 1992 Effect of a nonuniform magnetic field on a two-dimensional electron gas in the ballistic regime Phys. Rev. Lett. 68 385
6. Sheng D N and Weng Z Y 1995 Delocalization in a random magnetic field Phys. Rev. Lett. 75 2388
7. Avishai Y, Hatsugai Y and Kohmoto M 1993 Localization problem of a two-dimensional lattice in a random magnetic field Phys. Rev. B 47 9561
8. Xie X C, Wang X R and Liu D Z 1998 Kosterlitz–Thoulesstype metal–insulator transition of a 2D electron gas in a random magnetic field Phys. Rev. Lett. 80 3563
9. Mirlin A D, Polyakov D G and W¨olfle P 1998 Composite fermions in a long-range random magnetic field: Quantum Hall effect versus Shubnikov–de Haas oscillations Phys. Rev. Lett. 80 2429
10. Mancoff F B, Clarke R M, Marcus C M, Zhang S C, Campman K and Gossard A C 1995 Magnetotransport of a two-dimensional electron gas in a spatially random magnetic field Phys. Rev. B 51 13269
11. [11] Magier R and Bergman D J 2006 Strong field magnetotransport of two-phase disordered media in two and three dimensions: exact and approximate results Phys. Rev. B 74 094423
12. Bending S J, von Klitzing K and Ploog K 1990 Two-dimensional electron gases as a flux detector for a type II superconducting film Phys. Rev. B 42 9859
13. Geim A K, Bending S J and Grigorieva I V 1992 Asymmetric scattering and diffraction of two-dimensional electrons at quantized tubes of magnetic flux Phys. Rev. Lett. 69 2252 [14] Craik D 1997 Magnetism Principles and Applications (New York: Wiley)